Inorganic Chemistry

COMMUNICATION

pubs.acs.org/IC

Pyrazolylborates and Their Importance in Tuning Single-Molecule Magnet Properties of $\{Fe^{III}_2Ni^{II}\}$ Complexes

Yuan-Zhu Zhang,[†] Uma P. Mallik,[†] Nigam P. Rath,[†,‡] Rodolphe Clérac,*[,§,⊥] and Stephen M. Holmes*[,†,‡]

[†]Department of Chemistry & Biochemistry and [‡]Center for Nanoscience, University of Missouri—St. Louis, St. Louis, Missouri 63121, United States

[§]CNRS, UPR 8641, Centre de Recherche Paul Pascal, Equipe "Matériaux Moléculaires Magnétiques", 115 Avenue du Dr. A. Schweitzer, Pessac 33600, France

[⊥]Université de Bordeaux, UPR 8641, Pessac 33600, France

Supporting Information

ABSTRACT: A new tricyanoferrate(III) building block and a trinuclear single-molecule magnet derivative are described. The treatment of a 2:1 ratio of $[NEt_4][(Tp^{*Bn})Fe^{III}(CN)_3]\cdot H_2O\cdot MeOH$ [**1**; Tp^{*Bn} = tris(3,5-dimethyl-4-benzyl)pyrazolylborate] with nickel(II) trifluoromethanesulfonate gives $\{[(Tp^{*Bn})Fe^{III}(CN)_3]_2[Ni^{II}(DMF)_4]\}\cdot 2DMF$ (**2**; DMF = *N*,*N*-dimethylformamide). The symmetry-equivalent Fe^{III}_{LS} ions lead to a favorable alignment of anisotropy tensors (i.e., Fe···B axes) in **2**, and an energy barrier of Δ_{eff}/k_B = 16.7 K is found for the S_T = 2 complex.

Single-molecule magnets (SMMs) continue to receive considerable attention owing to their rich chemistry and ability to allow for detailed structure−property relationships to be described.[1] Among these nanomagnets are cyanometalate-based complexes, for which unquenched orbital angular momentum plays a crucial role in establishing an energy barrier to magnetization reversal.[1c,2−5] While several classes of cyanide-based SMMs have been reported, the vast majority utilizes $[(Tp^R)M^n(CN)_3]^{n-4}$ building blocks, where Tp^R is a tridentate poly(pyrazolyl)borate and M^{n+} is a trivalent (e.g., low-spin Fe^{III}) ion.[3−5]

Pyrazolylborates are ideal facially coordinate capping ligands because (i) they are known to stabilize a variety of metal oxidation states and (ii) they can be chemically modified at up to 10 positions, affording a systematic means for tuning electronic, steric demand, and solubility properties of derived complexes. The treatment of these tricyanometalate complexes with those containing substitutionally labile ligands allows for the construction of polynuclear entities, where the numbers and spatial orientations of the M(μ-CN)M′ formed units may be modulated at the molecular level. The pyrazolylborate ligands serve as invaluable tools for engineering polynuclear complexes that adopt quasi-predictable structural topologies of a given nuclearity.[3−5]

By changing the numbers and locations of aliphatic groups present on Tp^R ligands, we recently demonstrated that self-assembly reactions may be controlled and selectively afford cubic[3e] and rod-shaped[3d] $\{Fe^{III}_4Ni^{II}_4\}$ complexes. Surprisingly, the connectivity and spatial arrangement of Ni^{II} and Fe^{III}_{LS} ions, with Tp^{*Me} [tris(3,4,5-trimethyl(pyrazol-1-yl)borate], lead to a low-symmetry complex with a rather large SMM energy barrier (Δ/k_B = 33 K) for cyanide-based complexes.[3d] In comparison, smaller tetra(pyrazol-1-yl)borate [pzTp] ligands afford higher-symmetry cubic analogues ($\Delta/k_B \sim 12$ K),[3a] suggesting that a favorable alignment of anisotropy local tensors is operative in the former case. In an effort to further investigate this hypothesis, we elected to modify the magnetic behavior of trinuclear S_T = 2 $\{Fe^{III}_2Ni^{II}\}$ complexes in terms of their overall spin ground state (using para- and diamagnetic ancillary ligands) and spatial arrangement of $Fe^{III}(\mu$-CN)Ni^{II} linkages (*cis* vs *trans*). Of the known $\{Fe^{III}_2Ni^{II}\}$ complexes,[3b,6] only one is reported to be an SMM.[3b] We now describe recent efforts aimed at modifying the magnetic behavior of trinuclear SMMs by tuning the steric demand of ancillary ligands present.

The dropwise addition of a 1:1 dimethylformamide/acetonitrile (DMF/MeCN) solution of KTp^{*Bn} [where Tp^{*Bn} = tris(3,5-dimethyl-4-benzyl)pyrazolylborate] into iron(II) acetate in DMF afforded a gray mixture that was evacuated to dryness, extracted into MeCN, and added dropwise to a MeCN solution of $[NEt_4]CN$. The oxidation of the tricyanoferrate(II) complex was accomplished via the addition of hydrogen peroxide.[7] The IR spectrum of $[NEt_4][(Tp^{*Bn})Fe^{III}(CN)_3]\cdot H_2O\cdot MeOH$ (**1**) contains intense $\bar{\nu}_{BH}$ (2521 cm^{-1}) and $\bar{\nu}_{CN}$ (2119 cm^{-1}) absorptions[7] that are consistent with the presence of a trivalent iron.[3,4,8]

Compound **1** crystallizes in the monoclinic *C*2/*c* space group (Figure S1 in the Supporting Information, SI).[7] The structure of **1** shows benzyl groups that are approximately related via a 3-fold rotation about the B1···Fe1 axis and adopt a propeller-like orientation, leading to quasi-C_3 symmetry for the $[(Tp^{*Bn})Fe^{III}(CN)_3]^-$ anion. The average Fe−C and Fe−N bonds [1.921(3) and 2.000(2) Å] and the C−Fe1−C and N−Fe1−N angles [88.806(1) and 89.317(1)°] are typical of those seen for a range of $[(Tp^R)Fe^{III}(CN)_3]^-$ anions.[3,4]

The treatment of **1** with $Ni^{II}(OTf)_2$ (OTf = trifluoromethanesulfonate) in DMF in a 2:1 ratio affords red crystals of $\{[(Tp^{*Bn})Fe^{III}(CN)_3]_2[Ni^{II}(DMF)_4]\}\cdot 2DMF$ (**2**) within 7 days. The IR spectrum of **2** contains strong $\bar{\nu}_{BH}$ (2537 cm^{-1}) and $\bar{\nu}_{CN}$ (2174 and 2118 cm^{-1}) absorptions, indicating that bridging and terminal cyanides are present.[2d,3,4,7,8] Surprisingly, the bridging cyanides (2174 cm^{-1}) are higher in energy than those seen for either trinuclear V-shaped $\{[(pzTp)Fe^{III}(CN)_3]_2[Ni^{II}(bpy)_2]\}\cdot 2H_2O$ (2162 cm^{-1}) and linear $\{[(pzTp)Fe^{III}(CN)_3]_2[Ni^{II}(1,5,8,12\text{-tetraazadodecane})]\}\cdot {}^1/_2MeOH$ (2137 cm^{-1})

Received: August 16, 2011
Published: September 27, 2011

dx.doi.org/10.1021/ic2017825 | *Inorg. Chem.* 2011, 50, 10537–10539

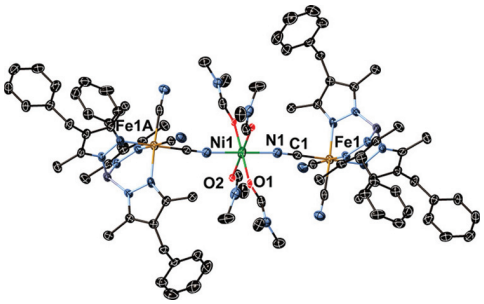

Figure 1. X-ray structure of **2**. Thermal ellipsoids are at the 50% level, and all hydrogen atoms and the lattice solvent are eliminated for clarity. Selected bond distances (Å) and angles (deg): Fe1−C1 1.888(4), Ni1−N1 2.007(3); C1−Fe1−C2 85.9(1), N1−Ni1−O1 90.1(1), Fe1−C1−N1 178.8(3), Ni1−N1−C1 173.3(3).

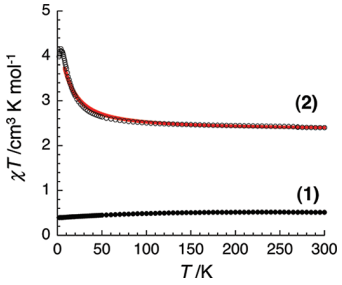

Figure 2. χT vs T data for **1** and **2** at 1000 Oe (with χ defined as the magnetic susceptibility and equal to M/H). Solid red line represents the best simulation for **2** down to 8 K as described in the text.

complexes, suggesting that efficient depopulation of the weakly antibonding cyanide 5σ orbital is operative in **2**.[3b,8]

Compound **2** crystallizes as a linear trinuclear complex in the triclinic $P\bar{1}$ space group (Figure 1).[7] The structure of **2** contains a central $\{trans\text{-}Ni^{II}(DMF)_4\}^{2+}$ unit that is linked to two adjacent and symmetry-related $[(Tp^{*Bn})Fe(CN)_3]^-$ anions. The bridging Fe−C_{CN} bonds [Fe1−C1, 1.888(4) Å] are slightly shorter than the terminal ones [1.925(4) and 1.926(3) Å], while the Fe−C1−N1−Ni unit is nearly linear, with Fe1−C1≡N1 and Ni1−N1≡C1 bond angles of 178.8(3) and 173.3(3)°, respectively. The slightly distorted Ni^{II} ion displays Ni−O [Ni−O1, 2.075(2) Å] and Ni−N_{CN} [Ni1−N1, 2.007(3) Å] distances that compare favorably to those in polynuclear $\{Fe^{III}{}_nNi^{II}{}_m\}$ complexes.[3,4]

The static and dynamic magnetic properties of **1** and **2** have been measured between 1.8 and 300 K. The room temperature χT value for **1** (0.52 cm^3 K mol^{-1}) is consistent with the presence of magnetically isolated ions with an orbital contribution to its $S = {}^1/_2$ spin state, thus leading to $g = 2.35$ (Figures 2 and S2 and S3 in the SI).[7] For **2**, the χT value at 300 K (2.5 cm^3 K mol^{-1}) suggests that a 2:1 ratio of magnetically isolated $Fe^{III}{}_{LS}$ ($S = {}^1/_2$; $2.6 \le g \le 2.8$) and Ni^{II} ($S = 1$; $2.0 \le g \le 2.2$) ions is present.[3,4] With cooling (Figure 2), the χT product increases and reaches a maximum value of 4.20 cm^3 K mol^{-1} at 4.0 K, as expected when the dominant interactions between $Fe^{III}{}_{LS}$ and Ni^{II} spin carriers are ferromagnetic; below 4 K, the χT value approaches a minimum (3.97 cm^3 K mol^{-1}) at 1.8 K. Considering the trinuclear structure of **2**, the χT versus T data were initially fitted using an isotropic Heisenberg Hamiltonian model in a weak-field approximation (eq 1), where J represents an isotropic interaction between $Fe^{III}{}_{LS}$ and Ni^{II} sites and S_i is the

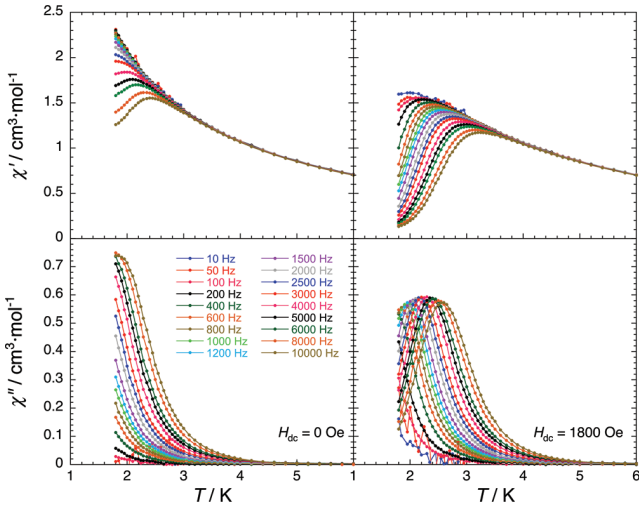

Figure 3. In-phase (χ') and out-of-phase (χ'') components of the ac susceptibilities for **2** for $H_{dc} = 0$ (left) and 1800 Oe (right) [$H_{ac} = 1$ Oe].

spin operator for each metal ion ($S_{Ni} = 1$; $S_{Fe1} = S_{Fe1A} = {}^1/_2$).[4c] To minimize contributions arising from magnetic anisotropy and intercomplex interactions, the magnetic susceptibility has been fitted above 8 K, with values of $J/k_B = +7.1(2)$ K and $g = 2.3(1)$ (Figure 2) indicating an $S_T = 2$ ground state for **2**. It is worth mentioning that the obtained ferromagnetic interaction, J, and g values are comparable to those reported for cyano-based Fe^{III}/Ni^{II} complexes containing $[(Tp^R)Fe^{III}(CN)_3]^-$ anions.[3,6] Unfortunately, as is observed in related systems, attempts to incorporate different g factors and single-ion anisotropy (for Fe^{III} and Ni^{II}) did not significantly improve the quality of the simulation at low temperatures, suggesting that all or a combination of these factors are manifested below 8 K.

$$H = -2J[S_{Ni}(S_{Fe1} + S_{Fe1A})] \quad (1)$$

The M versus H data collected for **2** below 10 K (Figure S4 in the SI)[7] confirm that an anisotropic $S_T = 2$ spin ground state is present. The magnetization does not saturate (up to 7.0 T and 1.8 K) and reaches a maximum value of 3.8 μ_B, which is lower than that predicted (4.6 μ_B) if $g = 2.3$ for an $S_T = 2$ magnetic ground state. Assuming that significant uniaxial magnetic anisotropy is present, the M versus HT^{-1} data for **2** were tentatively fitted using a macrospin model ($S_T = 2$) using the Hamiltonian $H = DS_{T,z}{}^2$. Unfortunately, this approach leads to unrealistic magnetic parameters ($D/k_B < -10$ K), suggesting that the magnetic ground state is not exclusively populated even at 1.8 K. It is also worth noting that no M versus H hysteresis is detected above 1.8 K.

The magnetic property dynamics of **2** have been studied using alternating-current (ac) susceptibility measurements obtained at various frequencies and temperatures. The ac data are strongly frequency-dependent in both in-phase (χ') and out-of-phase (χ'') components at $H_{dc} = 0$ Oe (Figures 3 and S5 in the SI),[7] clearly indicating that **2** exhibits dynamic behavior consistent with slow relaxation of magnetization exhibited by a SMM. The temperature dependence of the relaxation time (τ) of **2** cannot be accurately deduced from these ac data because of the absence of a maximum value in χ'' over a reasonable range of frequencies and temperatures (i.e., a maximum of χ'' is only observed at 1.80, 1.85, and 1.9 K: 7700, 8500, and 9500 Hz, respectively; Figure S5 in the SI).

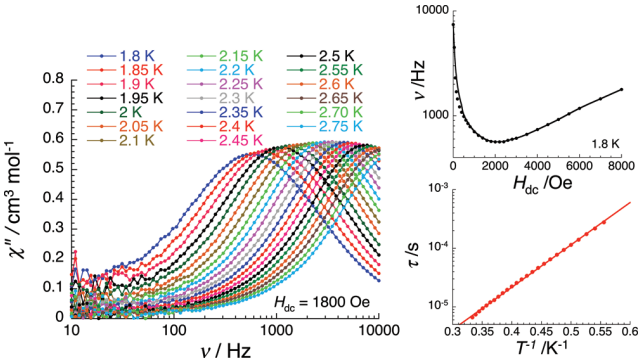

Figure 4. Frequency dependence of the out-of-phase (χ'', left) component of the ac susceptibility between 1.8 and 2.75 K (H_{ac} = 1 Oe; H_{dc} = 1800 Oe) for **2**. Insets: (top) ν vs H data for **2** at 1.8 K. The solid line is a guide. (bottom) Semilogarithmic τ vs $1/T$ plot from the frequency dependence of the ac susceptibility at H_{dc} = 1800 Oe for **2**. The red line represents the best fit of the τ vs $1/T$ data to the Arrhenius law.

Nevertheless, the fast relaxation of magnetization observed for **2** might be the result of the combined effects of thermally activated and quantum relaxation pathways. In order to verify that quantum tunneling of magnetization (QTM) is operative, additional ac measurements were initiated under small direct-current (dc) fields ($H_{dc} \leq 8$ kOe). If QTM is an efficient pathway of magnetization relaxation in **2**, small dc fields are expected to lift the degeneracy of the $\pm m_S$ states, decrease the probability of quantum tunneling, and thus increase the observed relaxation time.[3,4] Indeed, the application of dc fields causes a dramatic reduction of the characteristic frequency (maximum in the χ'' vs ν data) from 7500 Hz (at H_{dc} = 0 Oe) to a minimum value of 570 Hz at ca. 1800−2200 Oe (see Figure S6 in the SI and the inset of Figure 4). At this optimum field (where QTM probability is minimized), ac data have been measured (Figures 4 and S7 in the SI) and the temperature dependence of the relaxation deduced (inset of Figure 4). As expected, the relaxation time follows Arrhenius behavior, with $\tau_0 = 2.8 \times 10^{-8}$ s and an effective energy barrier of 17 K found (inset of Figure 4), being within the typical ranges seen for a variety of cyanide-based SMMs.[2−4] Considering that an effective energy barrier of 17 K and that only the S_T = 2 ground state is thermally populated below 2.75 K, a crude and minimum estimation of the uniaxial anisotropy term is $D/k_B \approx -4.2$ K for **2**.

The magnetic properties of **2** resemble those seen for $\{[(pzTp)Fe^{III}(CN)_3]_2[Ni^{II}(bipy)_2]\}\cdot 2H_2O$, which has a very different spatial arrangement of $Fe^{III}(\mu\text{-}CN)Ni^{II}$ units (*cis* vs *trans*).[3b] Interestingly, the common structural feature between these two complexes is the relatively good alignment (due to mirror and inversion symmetry, respectively) of the pseudo-C_3 anisotropy axes (B1···Fe1) of the two trivalent iron centers, which leads to significant uniaxial anisotropy (Figure S8 in the SI). In both complexes, the Fe^{III}_{LS}−CN−Ni^{II} units are nearly linear, allowing an efficient and comparable exchange interaction (7.1 vs 7.0 K) to thermally stabilize the S_T = 2 ground state. As a result of both the uniaxal anisotropy and well-defined ground states in the temperature range for which the slow relaxation is observed, the differences in effective energy barrier values (17 vs 20.6 K) are small. This work highlights the key role of the ancillary ligands and, in particular, their steric demand, in tuning the symmetry and spatial arrangement of anisotropic molecular building blocks present in polynuclear complexes.

■ ASSOCIATED CONTENT

Supporting Information. X-ray crystallographic data in CIF format, experimental details, and additional magnetic data. This material is available free of charge via the Internet at http://pubs.acs.org.

■ AUTHOR INFORMATION

Corresponding Author

*E-mail: clerac@crpp-bordeaux.cnrs.fr (R.C.), holmesst@umsl.edu (S.M.H.).

■ ACKNOWLEDGMENT

S.M.H. gratefully acknowledges the National Science Foundation (Grant CHE 0914935, CAREER; Grant CHE 0939987, X-ray upgrade) and the University of Missouri—St. Louis for financial support. R.C. acknowledges the University of Bordeaux, the ANR (NT09_469563, AC-MAGnets project), the Région Aquitaine, the GIS Advanced Materials in Aquitaine (COMET Project), and the CNRS (PICS N°14659) for financial support.

■ REFERENCES

(1) (a) Gatteschi, D.; Sessoli, R. *Angew. Chem., Int. Ed.* **2003**, *42*, 268−297 and references cited therein. (b) Beltran, L. M. C.; Long, J. R. *Acc. Chem. Res.* **2005**, *38*, 325−334 and references cited therein. (c) Shatruk, M.; Avendano, C.; Dunbar, K. R. *Prog. Inorg. Chem.* **2009**, *56*, 273−279 and references cited therein.

(2) (a) Sokol, J. J.; Hee, A. G.; Long, J. R. *J. Am. Chem. Soc.* **2002**, *124*, 7656–7657. (b) Berlinguette, C. P.; Vaughn, D.; Canada-Vilalta, C.; Gálan-Mascarós, J. R.; Dunbar, K. R. *Angew. Chem., Int. Ed.* **2003**, *42*, 1523–1526. (c) Song, Y.; Zhang, P.; Ren, X.-M.; Shen, X.-F.; Li, Y.-Z.; You, X.-Z. *J. Am. Chem. Soc.* **2005**, *127*, 3708–3709. (d) Li, D. F.; Parkin, S.; Wang, G. B.; Yee, G. T.; Prosvirin, A. V.; Holmes, S. M. *Inorg. Chem.* **2005**, *44*, 4903–4905. (e) Schelter, E. J.; Karadas, F.; Avendano, C.; Prosvirin, A. V.; Wernsdorfer, W.; Dunbar, K. R. *J. Am. Chem. Soc.* **2007**, *129*, 8139–8149. (f) Freedman, D. E.; Jenkins, D. M.; Iavarone, A. T.; Long, J. R. *J. Am. Chem. Soc.* **2008**, *130*, 2884–2885. (g) Zhang, Y.-Z.; Wang, B.-W.; Sato, O.; Gao, S. *Chem. Commun.* **2010**, *46*, 6959–6961.

(3) (a) Li, D. F.; Parkin, S.; Wang, G. B.; Yee, G. T.; Clérac, R.; Wernsdorfer, W.; Holmes, S. M. *J. Am. Chem. Soc.* **2006**, *128*, 4214–4215. (b) Li, D.-F.; Clérac, R.; Parkin, S.; Wang, G.-B.; Yee, G. T.; Holmes, S. M. *Inorg. Chem.* **2006**, *45*, 5251–5253. (c) Li, D.-F.; Clérac, R.; Wang, G.; Yee, G. T.; Holmes, S. M. *Eur. J. Inorg. Chem.* **2007**, 1341–1346. (d) Zhang, Y.-Z.; Mallik, U. P.; Rath, N.; Yee, G. T.; Clérac, R.; Holmes, S. M. *Chem. Commun.* **2010**, *46*, 4953–4955. (e) Zhang, Y.-Z.; Mallik, U. P.; Clérac, R.; Rath, N.; Holmes, S. M. *Chem. Commun.* **2011**, *47*, 7194−7196.

(4) (a) Wang, C.-F.; Zuo, J.-L.; Bartlett, B. M.; Song, Y.; Long, J. R.; You, X.-Z. *J. Am. Chem. Soc.* **2006**, *128*, 7162–7163. (b) Jiang, L.; Choi, H. J.; Feng, X.-L.; Lu, T.-B.; Long, J. R. *Inorg. Chem.* **2007**, *46*, 2181–2186. (c) Wang, C.-F.; Liu, W.; Song, Y.; Zhou, X.-H.; Zuo, J.-L.; You, X.-Z. *Eur. J. Inorg. Chem.* **2008**, 717–727. (d) Wu, D.-Y.; Zhang, Y. J.; Huang, W.; Sato, O. *Dalton Trans.* **2010**, *39*, 5500–5503.

(5) Park, K.; Holmes, S. M. *Phys. Rev. B* **2006**, *74*, 224440.

(6) (a) Wang, S.; Zuo, J.-L.; Zhou, H.-C.; Song, Y.; You, X.-Z. *Inorg. Chim. Acta* **2005**, *358*, 2101–2106. (b) Wang, C.-F.; Gu, Z.-G.; Lu, X.-M.; Zuo, J.-L.; You, X.-Z. *Inorg. Chem.* **2008**, *47*, 7957–7959. (c) Gu, J.-Z.; Jiang, L.; Tan, M.-Y.; Lu, T.-B. *J. Mol. Struct.* **2008**, *890*, 24–30.

(7) See the Supporting Information.

(8) Nakamoto, K. *Infrared and Raman Spectra of Inorganic and Coordination Compounds*, 5th ed.; Wiley: New York, 1997; Part B, pp 54−58, 105−116.